International Journal of Concrete Structures and Materials

RESEARCH Open Access

Effectiveness of Biological Mortars with Bacterial Glycocalyx on Service Life of Concrete Structures Exposed to Salt Attack

Hyun-Sub Yoon[6], Keun-Hyeok Yang[1*], Seung-Jun Kwon[2], Ji-Won Hwang[3], Sang-Seob Lee[4] and Nguyen Van Tuan[5*]

Abstract

This study investigated the effectiveness and limitations of newly developed biological mortars regarding chloride ion diffusion resistance. Through several tests on the glycocalyx production capacity and growth potentials of bacteria cells under marine environments, *Bacillus licheniformis* was isolated and immobilized in the expanded vermiculites together with a bacterial culture medium for producing biological mortars. The chloride ion diffusion coefficient of the mortars up to 91 days was determined through natural diffusion cell tests. Subsequently, the service life of RC structure repaired with biological mortars under chloride attack was evaluated considering multilayer theory and time-dependent diffusion. The addition of expanded vermiculites immobilizing *Bacillus licheniformis* significantly reduced the chloride ion diffusion coefficient. When its addition increased from 10 to 30%, the chloride ion diffusion coefficient decreased by 50–90% compared to that of mortars without bacteria. The service life of reinforced concrete structures repaired with biological mortars containing 30% expanded vermiculite concentration and thickness of 50 mm was evaluated to be six times longer than that of repaired with conventional mortar. Overall, this novel approach holds significant potential in addressing the salt-induced deterioration challenges faced by RC structures.

Keywords Biological mortar, Glycocalyx, Chloride ion diffusion coefficient, Service life

1 Introduction

Chloride-induced corrosion of reinforcing bars strongly affects safety of concrete structures exposed to marine environments or deicing chemicals. The strong alkalinity of the cement matrix in a reinforced concrete (RC) structure induces the formation of a passive layer of iron oxide on the surface of the reinforcing bar, which lowers its corrosion feasibility significantly and prevents its progress (Broomfield, 1997; Jung et al. 2018; Kwon et al. 2009). However, the intrusion of chloride ion leads to the local failure of the passive layer, which initiates corrosion. The service life of RC structures under chloride ingress condition is usually defined as the time at which the critical chloride concentration which can cause corrosion reaches the surface of the reinforcing bars (Nguyen et al., 2017; Yang et al. 2017).

Journal information: ISSN 1976-0485 / eISSN 2234-1315.

*Correspondence:
Keun-Hyeok Yang
yangkh@kgu.ac.kr
Nguyen Van Tuan
tuannv@huce.edu.vn
[1] Department of Architectural Engineering, Kyonggi University, Suwon, South Korea
[2] Department of Civil and Environmental Engineering, Hannam University, Daejeon, South Korea
[3] Department of Architectural Engineering, Kyonggi University Graduate School, Suwon, South Korea
[4] Department of Integrative Biotechnology, Sungkyunkwan University, Suwon, South Korea
[5] Faculty of Building Materials, Hanoi University of Civil Engineering, Hanoi, Vietnam
[6] Korea Disaster Prevention Safety Technology Co., Seoul, South Korea

To prevent the corrosion of the reinforcing bars, the effect of chloride on concrete can be controlled by applying the following engineering techniques (Petcherdchoo et al. 2015; Scarfato et al. 2012; Yoon et al. 2021; Yuan et al. 2017): (1) reducing the concentration of free chloride in concrete where the reinforcing bars are located; (2) retarding the penetration of chloride into concrete by controlling the its flux; (3) inducing the formation of binding salts like Friedel's salts, to densify the cement matrix structure for enhancing durability and delay of diffusion. The above techniques can be adopted to an undamaged concrete structure before it is exposed to chloride attack to delay its deterioration. However, in structures that have been exposed to marine environments or deicing chemicals for a long time, the chloride concentration at the reinforcing bar surface may reach the chloride threshold due to its diffusion or convection. Deterioration phenomena, such as cracking and delamination of the surface concrete owing to the swelling of the reinforcing bars, have been frequently observed in such structures (Shaikh, 2018). As a usual, restoring the concrete that has been suffered from cracking and delamination requires rehabilitation with anti-rust treatment. Surface coating techniques employing organic solvents or salt-resistant concrete containing blast furnace slag or fly ash are widely used for protecting concrete. Surface coatings with organic surface layer physically block the chloride penetration from the concrete surface, thereby significantly improving the impermeability of the concrete (Diamanti et al. 2013). However, using organic solvents needs frequent repairs of the concrete structure due to the defects caused by material heterogeneity in the structure. In view of economic feasibility, organic-solvent layers applied to impart impermeability to concrete surfaces have a relatively small thickness of 1–2 mm; hence, weathering and physical erosion are commonly observed in offshore structures moored in relatively severe environments, such as breakwaters (Wetzel et al. 2006; Woo et al. 2008). Salt-resistant concrete mixtures containing blast furnace slag or fly ash can improve the chloride-binding capacity of cement-based concrete, thereby delaying chloride penetration and reducing free chloride content (Arya et al. 1990; Arya & Xu, 1995; Dhir et al. 1997; Luo et al. 2003; Petcherdchoo et al. 2015). The formation of Al_2O_3-Fe_2O_3 mono (AFm) phase increases when salt-resistant concrete is mixed with blast furnace slag or fly ash due to the high Al_2O_3 content, which can improve the chloride-binding capacity and delay chloride penetration (Yuan et al. 2009). The AFm phase may initially exhibit a high chloride adsorption capacity; however, it depends on the chemically equivalent compounds produced through the reaction of the AFm phase and chlorides, bound as insoluble compounds, such as Friedel's salt (Yoon et al. 2021).

Most maintenance techniques with bacteria employed for improving the impermeability of concrete or controlling the penetration of corrosive agents focus on crack healing using calcium carbonate precipitated by bacteria (Qian et al. 2021; Wang et al. 2016). Although crack-healing techniques and the chloride-control techniques described previously share the same purpose, the applications of these techniques differ in principle. The former is intended to heal cracks unavoidably caused by the temperature-induced expansion, contraction of concrete, and excessive load during maintenance, and control the penetration of corrosive species into the cracks. There are some local limitations to applying crack healing to concrete structures exposed to deteriorating conditions, regardless of the extent of the damaged and undamaged parts, so that achieving a better control of chloride penetration in concrete or mortar is difficult for the purpose of crack healing (Zahn et al. 2022). Several studies presented a technique for improving the durability of concrete using glycocalyx, a biofilm formed by bacteria in an environment exposed to sulfates (Yang et al. 2018). Glycocalyx formed by bacteria was used as a protective body to control sulfate penetration. The resistance of the material, to which the strains were applied, against sulfuric acid degradation increased by 9–11 times compared to that of a conventional material (Yoon et al. 2022a, 2022b). By effectively sealing the concrete's porosity and providing an additional protective layer, biological mortars offer a sustainable and eco-friendly solution for enhancing the durability and extending the service life of concrete infrastructure in salt-laden environments.

In this study, a biological mortar with a high resistance to salt damage using glycocalyx generated by halophilic bacteria was newly developed. Considering the glycocalyx production capacity, growth, and propagation potential in a marine environment, *Bacillus licheniformis* was isolated and immobilized in expanded vermiculites together with a bacterial culture medium, following the immobilization technique employed in the previous work (Yoon et al. 2021). The compressive strength and chloride ion diffusion coefficient of mortars were examined considering the concentration of expanded vermiculite-immobilizing bacteria. The population of bacteria that survived in the hardened mortars exposed to NaCl solution having a concentration of 165 kg/m^3 was assessed using the viable cell count method (Freshney, 1987). Subsequently, the expected service life of the concrete repaired with the developed biological mortar was evaluated using multilayer diffusion theory and time-dependent penetration analysis in marine environments.

2 Experimental Details

2.1 Identification of Bacteria

The glycocalyx-forming halophilic bacteria were isolated from mussel shells found in Wando port, Cheonnam province, South Korea. The isolated bacteria were inoculated in a marine medium (Table 1) with a concentration of 3.5% NaCl and subsequently cultured under aerobic conditions at 28 ± 2 °C. The cultured bacterial strains were identified individually using 16s-rDNA sequence analysis through polymerase chain reaction of DNA chromosomes extracted using proteolytic enzyme treatment, and the distinct phenotypic characteristics were analyzed using a transmission electron microscope (TEM) (Imhoff et al. 1984; Kawasaki et al. 1993; van Niel 1994; Willems et al. 1991). The DNAs of the strains were compared with the bacterial sequence database from the US National Center for Biotechnology Information using a microbial phylogenetic tree-analysis tool (Table 2). The TEM analysis was conducted based on Brenner et al. (2005)'s technique for observing bacterial cell size, morphology, and motility. Fig. 1 shows the TEM images of bacteria cells incubated in a marine media for 7 days. Using the aforementioned indicators, the isolated strains could be identified as *Bacillus licheniformis* (HY072501), as determined from the phylogenetic tree (Fig. 2). *Bacillus licheniformis* cells were rod shaped with lengths of 2.5–3.5 μm. This bacterium could be characterized as a gram-positive facultative anaerobe, indicating high tolerance to salinity, and good activity and growth over a wide range of temperatures.

Table 1 Characteristics of isolated slime forming halophilic bacteria

Characteristics	*Bacillus licheniformis* HY072501
Cell form	Rod
Cell size (μm)	(0.2-0.5)×(2.5-3.5)
Motility	+
Bacterial metabolism	Facultative aerobe
Gram staining	+
Denitrification	+
Color of cell suspension	Cream
Utilization of	
Succinate acid	+
D-Glucuronic acid	+
D-Galactose	−
D-Glucose	+
Stachyose	+
Methyl red test	−
Citrate test	−
Catalase test	+

Table 2 Results of *16s rDNA* sequencing analyses for isolated bacteria

Strain	Hit taxon name	Hit strain name	Accession number	Identities (%)
HY072501	*Bacillus licheniformis*	ATCC 14580(T)	AE017333	99.86%

Bacillus licheniformis is known to formulate glycocalyx on the outer cell skins to protect the cell and accelerate the interaction with other bacteria by blocking harmful substances that cause growth inhibition in an oxygen-deficient environment. The primary chemical components of glycocalyx are commonly accepted as mannose, rhamnose, glucosamine, galactose, phosphorus, and fatty acids (Yoon, 2021). Glycocalyx is composed of a sparse slime layer and polymer skin capsule that tightly surrounds a cell. The slime layer absorbs cations, including sodium (Na^+), calcium (Ca^{2+}), and magnesium (Mg^{2+}) and anions including chlorine (Cl^-) and sulfate (SO_4^{2-}), which are abundant in seawater, as nutrients necessary for the growth of bacteria. The physical immobilization of such ions by glycocalyx can be used for blocking penetration of free chloride ions from the concrete surface and thereby reduce the formation of soluble calcium chloride in the cement matrix. Hence, bacterial glycocalyx can serve as a protective barrier for mortars against the salt attack.

2.2 Cultivation and Immobilization of Isolated Bacteria

The main components of the MRS media, such as sodium chloride, proteose peptone, yeast extract, and sodium acetate, used to cultivate the isolated bacteria, are listed in Table 3. The sodium chloride was intended for emulating the salt concentration (approximately 3.5%) of seawater. The *Bacillus licheniformis* bacteria require a carbon source ($C_nH_nO_n$) to encourage the formation of glycocalyx under anaerobic conditions (Yoon, 2021). Hence, the amount of glycocalyx generated by the bacteria is significantly affected by the type

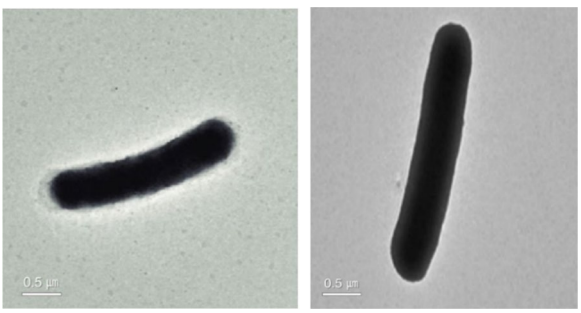

Fig. 1 TEM images of isolated bacteria

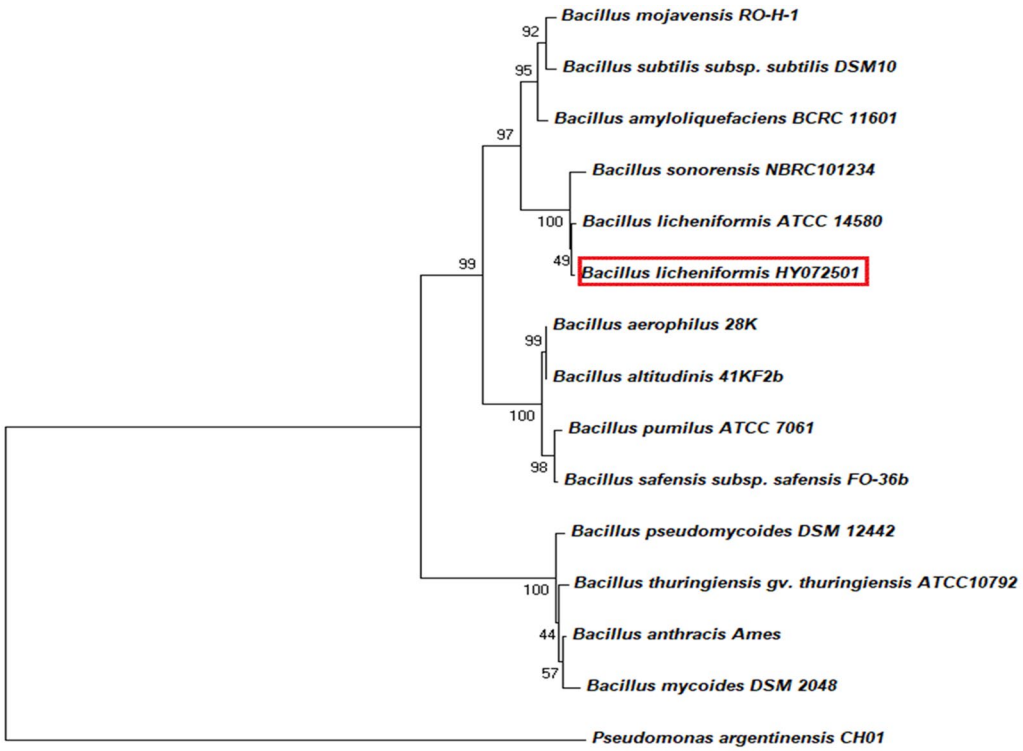

Fig. 2 Phylogenetic tree of isolated bacteria

Table 3 MRS media compositions for *Bacillus licheniformis*

Nutrients	Quantity
Proteose peptone No.3	5.0 g
Yeast extract	7.0 g
Ammonium citrate	1.0 g
Sodium acetate	2.5 g
Magnesium sulfate	0.1 g
Manganese sulfate	0.025 g
Di-potassium phosphate	1.0 g
Sodium chloride	35 g
Distilled water	1 L

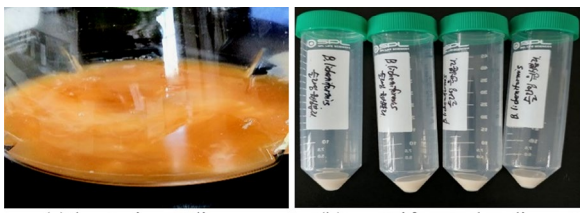

(a) bacteria medium (b) centrifugated sediment

Fig. 3 Images of cultivated bacteria medium and differentially centrifugated glycocalyx sediment

of carbon source that the bacteria have consumed as nutrients during its growth. In this study, glycocalyx formation was examined with respect to different carbon concentration of glycocalyx produced during the 24 h culture of the isolated bacteria was determined through centrifugation (7000 rpm/min, 7 min). Fig. 3 shows the typical images of bacteria medium and the various separated glycocalyx sediments. The *Bacillus licheniformis* produced more glycocalyx in glucose medium than in fructose or sucrose media. The glycocalyx concentration estimated in the glucose, fructose, and sucrose media were 0.95 g/l, 0.84 g/l, and 0.91 g/l, respectively. Hence, the glucose as the carbon source that encourage the formation of bacterial glycocalyx was selected. The cells were incubated at 28 ± 2 °C until the cell concentration reached 10^9 cell/ml. The cultivated bacteria were inoculated in a culture medium, in which chloride ions were removed through filtration. Subsequently, they were used for tests.

The expanded vermiculites in which the inoculated bacteria were immobilized had a porosity exceeding 50% and a density of 0.25 g/cm^3, as previously investigated by Yoon et al. (2022a, 2022b). The particle size of the expanded vermiculites varied between 0.25 and 0.36 mm. The immobilization of bacteria together with

the media in a porous material aims to improve the survival of the cells during mortar mixing and within the hardened cement matrix, and to elevate the activity of the bacteria even under a dry environment. The pores of the expanded vermiculates were impregnated with the concentrated bacterial suspension (concentration > 10^9 cells/ml) under a negative pressure environment of 10–20 torr in a sealed container. The negative pressure is generated by forcibly discharging the air in the pores inside the immobilization material. Fig. 4 shows the scanning electron microscope (SEM) images of the bacterial colonies and glycocalyx generated by the bacteria immobilized in the porous expanded vermiculites.

2.3 Biological Mortar Specimens

The biological mortars were prepared with the expanded vermiculites immobilizing the *Bacillus licheniformis* and MRS media. The amount of the expanded vermiculite for replacing fine aggregates by volume was the main test parameter, as given in Table 4. Hence, the mortar specimens were identified using the volume fraction of the expanded vermiculite, except for the control specimen (C) without the bacteria. For example, specimen BL-10 indicates a biological mortar prepared using 10% expanded vermiculite to the volume of fine aggregates.

The same mixture proportions were considered for all the mortar samples. The water-to-binder ratio and a fine aggregate-to-binder ratio were fixed at 0.35 and 2.0, respectively. Conventional ordinary Portland cement with a Blaine fineness of 3340 cm^2/g and density of 3.15 g/cm^3 was used as the main binder. Ethylene vinyl acetate (EVA) polymer was also added at 5% of the unit binder concentration to increase the bond strength of the mortars with the concrete surface. Natural silica sand with particle size varying between 0.17 and 0.7 mm was used as fine aggregates. No water-reducing agents were used in any of the mixtures.

The fresh mortars were cast into 50 mm cubic steel molds to test compressive strength at different ages and cast into cylindrical molds with a diameter of 100 mm and a height of 200 mm to examine the chloride ion diffusion coefficient. The cast mortars were cured at a room temperature of 20 ± 2 °C and relative humidity of 60 ± 5% for a specified age.

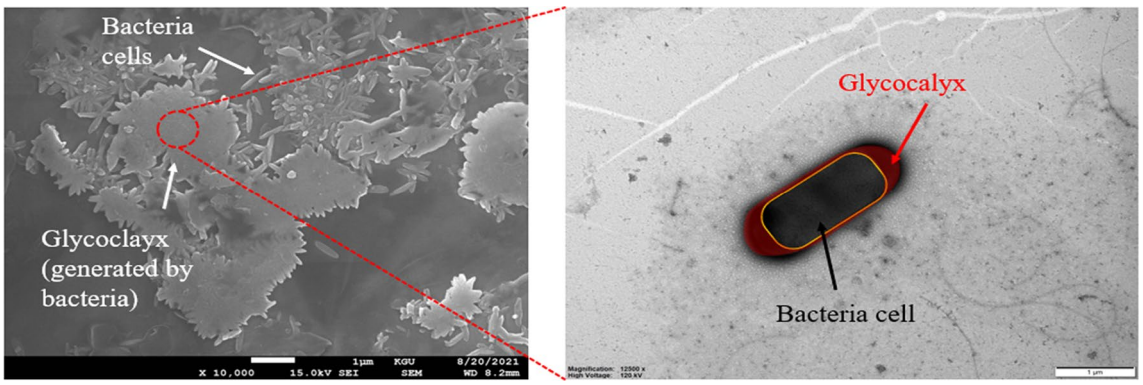

Fig. 4 Typical SEM and TEM images for bacterial colonies and glycocalyx immobilized in porous of expanded vermiculites

Table 4 Details of mixture proportions for mortar specimens

Specimens	Bacteria strain	R_E (%)	*W/B*	*S*/B	Unit weight (kg/m^3)				
					Water	Binder		EV	Silica sand
						OPC	EVA polymer		
C	–	0	0.35	2.0	262	675	75	–	1501
BL-10	*Bacillus licheniformis*	10			248	638	70	47	921
BL-20		20			233	600	66	44	867
BL-30		30			218	562	62	42	812

R_E = ratio of expanded vermiculite immobilizing bacteria and media as a replacement of silica sand by volume, *W/B* = water-to-binder ratio by weight, and *S/C* = silica sand-to-binder ratio by weight

OPC, EVA, and EV refer to ordinary Portland cement, ethylene vinyl acetate, and expanded vermiculite, respectively

2.4 Test of Strength and Chloride Diffusion

The compressive strength of the mortar was evaluated at 3, 7, 28, 56, and 91 days in accordance with the ASTM C109 (ACTM C109 2012) procedures. The chloride ion diffusion coefficient of the mortar was determined using the natural diffusion cell test method (Tritthart, 1989), which is more practical for simulating the chloride diffusion mechanism in an actual concrete structure exposed to salt attack than using a rapid chloride migration test with an electrical acceleration technique, although the former method requires long-term measurement (Wang & Fu, 2019). Note that the natural diffusion cell tests do not require applying current or voltage to measure the diffusion coefficient of chlorides. In addition, the electrical acceleration technique may yield too high chloride ion diffusion coefficients for mortar containing high porosity through a high electrical conductivity (Pontes et al. 2021). Fig. 5 shows the measuring set-up used for the natural diffusion cell test. The acrylic chamber was partitioned into two cells by a cylindrical mortar segment with a diameter of 100 mm and a height of 50 mm that was placed at the center of the chamber. The mortar segment was obtained from the cylinders cured at room temperature for 28 days. One cell was fully filled with distilled water and the other with NaCl solution at a concentration of 16.5 kg/m^3 (Yoon et al. 2022a, 2022b). The variation in chloride ion concentration up to 150 days was measured using LAQUA Bench top analyzer and a chloride ion electrode installed at each cell. When the chloride ion concentration profile is expressed as a function of time, the chloride ion diffusion coefficient (D_i) can be calculated using the following equation.

$$D_i = \frac{V\Delta Q}{A\Delta T} \times \frac{L}{c_1 - c_2} \tag{1}$$

where, V is the volume (m^3) of the diffusion cell, ΔQ is the increased chloride ion concentration (kg/m^3) in the cell containing distilled water, A is the exposed area (m^2) of the mortar segment (m^2), ΔT is the cumulative testing time (s) after the initialization, L is the thickness (m) of the mortar segment, c_1 is the chloride ion concentration in (kg/m^3) the cell containing NaCl solution, and c_2 is the chloride ion concentration (kg/m^3) of the cell containing distilled water.

The survival and activity of the bacteria were assessed by employing the viable cell count method (Yoon et al. 2022a, 2022b) using powder samples extracted from the mortar segments used for the natural diffusion cell test to simulate the exposure to the salt attack. The population of viable bacterial cells in the mortar segments was estimated quantitatively in accordance with the cell viability procedure (Yoon et al. 2021). The production of bacterial glycocalyx on the mortar segments was confirmed using SEM photographs. To observe the glycocalyx produced on the mortar surface, the samples were prepared for energy-filtering transmission electron microscopy.

2.5 Expected Service Life Assessment

The biological mortars developed in this study were primarily intended for repairing concrete damaged by chloride ingress. The repair mortars are placed after removal of the contaminated concrete surface; the renewal layer is a multilayer structure with a chloride ion diffusion coefficient different from that of the conventional layer to be repaired. Therefore, the chloride ion diffusion behaviors in the conventional and the newly repaired mortar layers were investigated (Yang et al. 2020a, 2020b). The chloride-penetration analysis model for a multilayer structure, based on Fick's 2nd Law, is expressed in Eq. (2). In a concrete structure, the porosity, ion concentration gradient, and chloride ion diffusion coefficient decrease with time after chloride exposure. Therefore, diffusion analysis in a multilayer considers the time-dependent penetration index of chloride ion diffusion from the aspect of multilayer diffusion theory (Andrade et al. 1997; Yoon et al. 2022a, 2022b).

$$\left\{ \begin{array}{l} C_1(x,t) = C_S \sum_{N=0}^{\infty} \alpha^n \left[erfc \left\{ \dfrac{2ne + x}{2\sqrt{\frac{D_1}{1-m}\left(\frac{t_0}{t}\right)^m t}} \right\} - \alpha \cdot erfc \dfrac{(2n+2)e - x}{2\sqrt{\frac{D1}{1-m}\left(\frac{t_0}{t}\right)^m t}} \right] \\ C_2 = \dfrac{2kC_S}{k+1} \sum_{N=0}^{\infty} \alpha^n erfc \left[\dfrac{(2n+1)e + k(x-e)}{2\sqrt{\frac{D_1}{1-m}\left(\frac{t_0}{t}\right)^m t}} \right] \end{array} \right\}, \quad (t < t_c) \tag{2}$$

$$\begin{cases} C_1(x,t) = C_S \sum_{N=0}^{\infty} \alpha^n \left[erfc\left\{ \dfrac{2ne+x}{2\sqrt{\frac{D_2}{1-m}\left(\frac{t_0}{t}\right)^m \left[1-m+m\left(\frac{t_c}{t}\right)\right]t}} \right\} \right. \\ \left. -\alpha \cdot erfc \dfrac{(2n+2)e-x}{2\sqrt{\frac{D_2}{1-m}\left(\frac{t_0}{t}\right)^m \left[1-m+m\left(\frac{t_c}{t}\right)\right]t}} \right] \\ C_2 = \dfrac{2kC_S}{k+1} \sum_{N=0}^{\infty} \alpha^n erfc \left[\dfrac{(2n+1)e+k(x-e)}{2\sqrt{\frac{D_1}{1-m}\left(\frac{t_0}{t}\right)^m \left[1-m+m\left(\frac{t_c}{t}\right)\right]t}} \right] \end{cases}$$

$(t \geq t_c)$

where, C_1 and C_2 are the chloride concentrations in the concrete surface and body (kg/m^3), respectively; D_1 and D_2 are the diffusion coefficients of the concrete surface and body (m^2/s), respectively; $k = (D_1 + D_2)^{1/2}$; $\alpha = (1-k)/(1+k)$; and e is the thickness of the surface reinforced through surface repair. The diffusion coefficient of the surface, D_1, was assumed to be smaller than the internal diffusion coefficient, C_2, to simulate the diffusion coefficient of a deteriorated concrete surface. In addition, m and t_c were assumed to be the time-dependent index of the diffusion coefficient and the time required for the diffusion coefficient to stabilize (30 years), respectively (Thomas & Bamforth, 1999; Thomas & Bentz, 2002).

Factors that affect the diffusion of chloride ions in a material include the related ion concentration, distance travelled, time of measurement, and temperature of the material. To apply the chloride ion diffusion coefficient to evaluate service life using the natural diffusion test method, the diffusion coefficient in a steady state is more reasonable (Tritthart, 1989; Yoon, 2021), so that the chloride ion diffusion coefficient of the biological mortar was evaluated after 91 days of the test start. The value of the chloride ion diffusion coefficient of conventional concrete was adopted from the previous results (Yang et al. 2020a, 2020b). For calculating the service life, 50 mm of concrete cover depth was assumed and the contained chlorides were cleanly removed from the surface of the concrete after completely removing the deteriorated parts of the concrete. According to the assumed conditions of the conventional layer, the thickness of the biological mortar was changed to 10 mm, 30 mm, and 50 mm, and the bacterial substitution ratio was adjusted accordingly. The service life was determined when the maximum chloride concentration on the surface of the reinforcement bar reaches 0.4% by binder mass as chloride threshold (Bagheri et al. 2021).

3 Test Results and Discussion

3.1 Compressive Strength Development

The results of compressive strength in biological mortar from 3 to 91 days are shown in Fig. 6. Test results are also summarized in Table 5. The compressive strength of the conventional mortar was the highest at all ages. Increasing the volume fraction of the expanded vermiculite containing immobilized *Bacillus licheniformis*, a halophilic glycocalyx-forming bacterium, slightly lowered the strengths of the biological mortars. The compressive strengths of the repair mortars substituted with 10% and

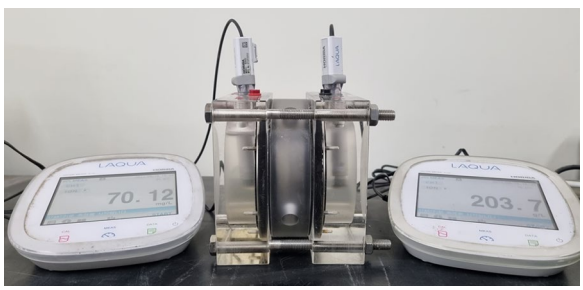

Fig. 5 Typical setting images of natural diffusion cell test

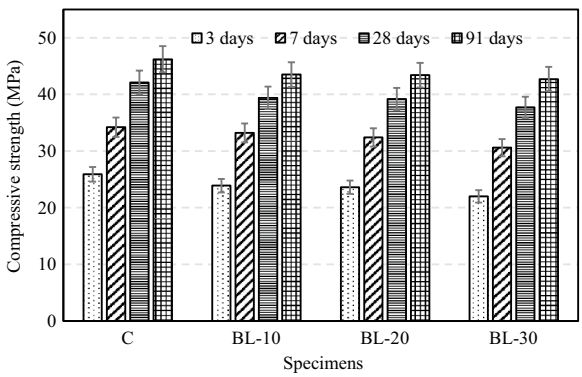

Fig. 6 Compressive strength of specimens at different ages

Table 5 Summary of test results on mortar specimens

Specimens	Compressive strength (MPa)				Chloride diffusion coefficient ($\times 10^{-12}$ m^2/s)			Bacteria cell population (cell/ml)
	3 days	7 days	28 days	91 days	56 days	91 days	150 days	91 days
C	25.9	34.2	42.1	46.2	1.62	1.45	1.32	–
BL-10	23.9	33.2	39.4	43.5	0.32	0.27	0.24	6.0×10^4
BL-20	23.6	32.4	39.2	43.4	0.22	0.18	0.15	8.5×10^4
BL-30	22.0	30.6	37.7	42.7	0.19	0.15	0.13	2.0×10^5

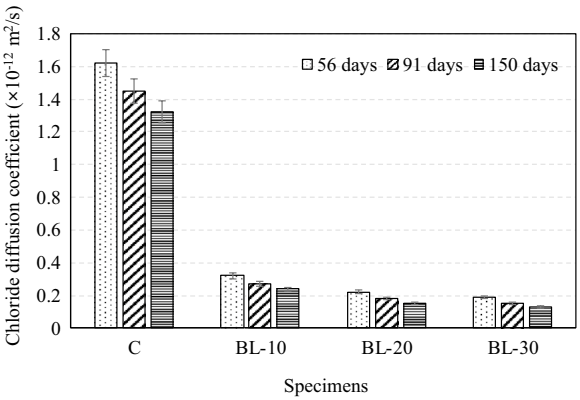

Fig. 7 Chloride diffusion coefficient of specimens at different ages

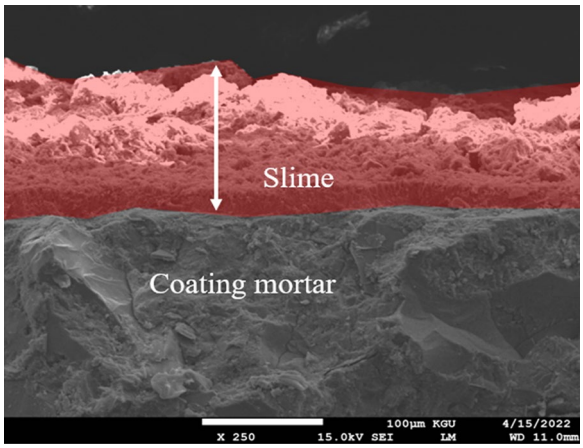

Fig. 8 Typical images of glycocalyx formed on the surface of biological mortar (magnified 250 times)

20% of expanded vermiculite measured at 28 days were 39.4 MPa and 39.2 MPa, respectively, which were only 6% lower than the compressive strength of the conventional mortar. The compressive strength of the BL-30 specimen, which had the highest substitution ratio of the porous expanded vermiculite, was the lowest of all specimens. The compressive strength of the BL-30 specimen was 37.7 MPa at 28 days, which was approximately 10% lower than that of the conventional mortar and those at the age of 91 days, the BL-30 specimen was also about 8% lower than that of the conventional mortar.

These results were obtained by 30% replacement of the total volume of aggregate with a porous material in the mortar mix and the strength reduction can be compensated through adjusting unit water content and *W/B* ratio.

3.2 Chloride Ion Diffusion Coefficient

The pore structure in cement matrix is getting densified with cement cluster expansion due to hydration reaction and the chloride ion diffusion coefficient also decreases with time (Riding et al. 2013), which have been reported in numerous investigations (Bagheri et al. 2021; Nokken et al. 2006; Riding et al. 2013; Thomas et al. 2020; Yang et al. 2020a, 2020b; Zhang et al. 2019). Wang and Fu (2019) reported that the physical definition of the apparent diffusion coefficient was the average of the chloride ion diffusion coefficient during the exposure period. The results obtained from the natural diffusion cell test can be assumed to be the apparent diffusion coefficient using the average of the chloride ion diffusion coefficient with respect to the exposure period. In other words, the chloride ion diffusion coefficients during the natural diffusion cells test are to be continuously collected at specific moments to determine the changes in the apparent diffusion coefficient. However, it takes months or years in this case, considering the chloride permeability and diffusion rate of the hardened cement in addition to the difficulties in maintaining the actual environmental conditions. Therefore, in this study, the chloride ion diffusion coefficient was evaluated from a short-term perspective based on the data of chloride ion concentration inside the spontaneous diffusion cell collected during the test at 56 days, 91 days and 150 days.

The chloride ion diffusion coefficients of the biological mortars estimated using natural diffusion experiments are shown in Fig. 7. The chloride ion diffusion coefficients of all specimens at 91 days decreased compared to that at 56 days and showed a marked difference with

the substitution ratio of the expanded vermiculite containing immobilized slime-forming bacteria. The chloride ion diffusion coefficient of the conventional mortar was the highest among all specimens, 1.62×10^{-12} m^2/s and 1.45×10^{-12} m^2/s at 56 days and 91 days, respectively. The reduction of the result with age in specimen C was approximately 10%. As can be seen from the details of the cement mixtures listed in Table 4, specimen C had a higher unit cement content, so that the improvement in the internal-structure densification with age and reduction of the chloride ion diffusion coefficient with reduction in chloride permeability were expected to be better in specimen C. However, the chloride ion diffusion coefficient of specimens mixed with glycocalyx-forming bacteria showed greater decreases compared to that of specimen C with increasing age. In addition, the chloride ion diffusion coefficient at all ages was lower than that of conventional cement mortar. At 91 days, the chloride ion diffusion coefficients of the repair mortar substituted with bacteria at 10% and 20% were 0.27×10^{-12} m^2/s and 0.18×10^{-12} m^2/s, respectively, which were much lesser than that at 56 days by 15% and 18%, respectively. At 91 days, the chloride ion diffusion coefficient of the repair mortar substituted with glycocalyx-forming bacteria at 30% was 0.15×10^{-12} m^2/s, which was approximately 89% lower than that of specimen C. In addition, the decreasing amount in the chloride ion diffusion coefficient with age was 21%, which was the largest among all specimens. This is because of the block effect of glycocalyx formed on the surface of the biological mortar on chloride penetration.

Fig. 8 shows the images of glycocalyx formation on the surface of specimen BL-30 exposed to NaCl solution with a concentration of 16.5 kg/m^3 for 91 days. The thickness of glycocalyx was estimated to be approximately 150 μm. Glycocalyx can be formed at the mortar surface through bacterial activity, which plays a role in blocking the penetration and diffusion of chloride ions into the mortar. The results from 150-day test showed similar trend with those from 56 to 91 days, however, the reduction ratio with increasing period was insignificant. The reduction ratio of chloride diffusion with time in biological was greater than that of conventional mortar. At the age of 150 days, chloride diffusion coefficient in conventional mortar was 1.32×10^{-12} m^2/s, which showed 9% of reduction ratio to 91-day result but B1-30 showed 13% of reduction ratio from 91 to 150 days. The reduction ratio amounted to 60% of the result from 56 to 91 days. Considering the non-linearly decreasing behavior of chloride diffusion with time, chloride diffusion coefficient in conventional mortar can be estimated. That in biological mortar shows low level of chloride diffusion at the initial period so that the reduction of chloride diffusion was small with time.

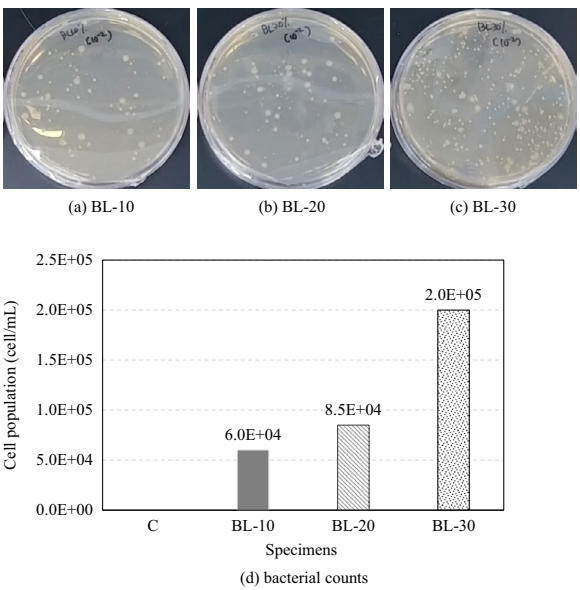

Fig. 9 Bacterial colonies and cell population counts results from the hardened mortars exposed to NaCl solutions for 91 days

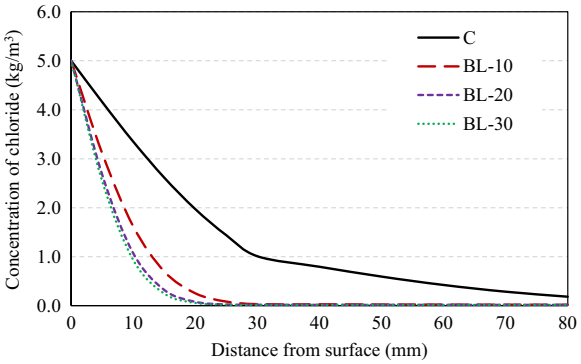

Fig. 10 Analytical chloride ion concentration profiles in the concrete structures repaired using mortar specimens at a thickness of 30 mm

Table 6 Parameters considered in the chloride-penetration analysis model (Eq. 2)

Specimens	Parameters in Eq. (2)			
	C_s (kg/m^3)	D_1 (m^2/s)	D_2 (m^2/s)	m
C	5	1.32×10^{-12}	3.5×10^{-12}	0.2
BL-10	5	0.24×10^{-12}	3.5×10^{-12}	0.2
BL-20	5	0.15×10^{-12}	3.5×10^{-12}	0.2
BL-30	5	0.13×10^{-12}	3.5×10^{-12}	0.2

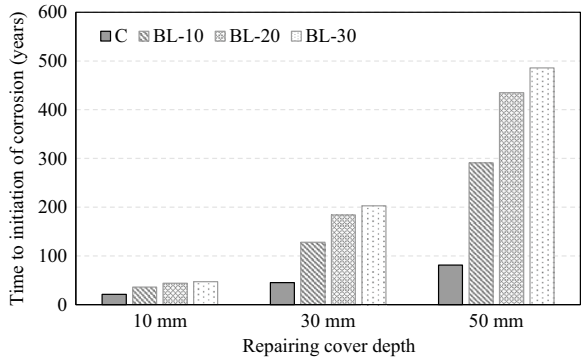

Fig. 11 Expected service life of concrete structures repaired using mortar specimens at different thicknesses

3.3 Survival Growth of Halophilic Glycocalyx-Forming Bacteria

Fig. 9 shows the images of the bacterial colonies and results of viable cell count of the bacteria cultured from biological mortar samples after natural diffusion cell test at 91 days. The viability of halophilic glycocalyx-forming bacteria showed a significant correlation with the chloride ion diffusion coefficient of the biological mortar evaluated previously. As the substitution ratio of the expanded vermiculite containing immobilized *Bacillus licheniformis* changed from 10 to 30%, the viable cell count of bacteria increased. The viable bacterial cell count in specimen BL-10 was 6.0×10^4 cells/ml and that of specimen BL-20 was 8.5×10^4 cells/ml, which was approximately 41% higher than that of specimen BL-10. The viable bacterial cell count in specimen BL-10 was 2.0×10^5 cells/ml, which was 1.4 times and 2.3 times higher than those of specimens BL-10 and BL-20, respectively. Considering the effect of substitution ratio of *Bacillus licheniformis* on chloride ion diffusion coefficient, increasing the bacterial substitution ratio is more effective for the formation of glycocalyx in the hardened mortar to improve the survival population and control the chloride penetration.

3.4 Service Life of Biological Mortar

Fig. 10 illustrates the time-dependent chloride ion diffusion behavior in a multilayer concrete structure repaired with biological mortar. This shows the profiles of chloride ion concentration in different types of mortar after 10 years; all repair mortars on the conventional layer were 30 mm thick. In this analysis, the repair structure was assumed to be exposed to harsh environment with salt-spraying to the concrete with 5 kg/m^3 of surface chlorides. The parameters considered in the chloride-penetration analysis model presented in Eq. (2) are listed in Table 6. The chloride ion concentration profile of the repair structure showed that in the biological mortar was significantly lower than that in conventional repair material. In particular, the chloride ion concentration in conventional repair materials at a depth of 30 mm from the surface was approximately 55 times higher than that in specimen BL-30.

Fig. 11 shows the results of the predicted service life with critical chloride content (0.4% by binder mass). The expected service life increased with increasing repair layer thickness; the difference from the calculating service life of the repair materials was even greater according to the increasing layer thickness. The service life of specimen C with 10 mm of the repair-layer thickness was the shortest at 21 years, followed by 45 years with 30 mm, and 81 years with 50 mm. The results of specimen BL-10 increased by 1.7 times, 2.8 times, and 3.6 times under a repair-layer thickness of 10 mm, 30 mm, and 50 mm, respectively, compared to that of specimen C. Compared to specimen C, specimen BL-20 showed a greater difference in expected service life with an increase in the repair layer thickness. A repair-layer thickness of 50 mm showed service life of 435 years, which was approximately 5.4 times longer than that of specimen C. From the assessment results on chloride ion diffusion coefficient, the expected service life of specimen BL-30, which was the shortest, became 486 years with increasing repair layer thickness to 50 mm, which was approximately six times longer than that of specimen C. Furthermore, the service life of specimen BL-30 was 2.2 times longer than that of specimen C even with a repair layer thickness of 10 mm.

With the same repair material, the increasing ratio of service life decreased when the repair-layer thickness firstly increased from 10 to 30 mm and then from 30 to 50 mm. The reduction amount was larger in the mix with a low chloride ion diffusion coefficient. When the repair-layer thickness of specimen C increased from 10 to 20 mm and then from 30 to 50 mm, the increasing ratio of service life increased by 214% and 180%, respectively. When the case of BL-10 firstly increased from 10 to 30 mm and then from 30 to 50 mm, it increased by 355% and 227%, respectively, which showed a decrease of 36% in the increasing ratio. As the case of BL-20 and BL-30 increased in the same manner, the service life increasing ratio decreased by 44% and 45%, respectively. As shown in Fig. 9, the repair material with a lower chloride ion diffusion ion coefficient showed a greater decrease in the chloride ion concentration from the surface so that chloride ions deep inside the concrete exhibit an insignificant difference even with an increase in the repairing thickness.

4 Conclusions

The aim of the study was to evaluate the chloride ion diffusion coefficient of biological mortars using glycocalyx-forming bacteria that inhibited the permeation and diffusion of chloride ions in structures exposed to marine environment. As further advancements are made in this field, it is expected that biological mortars will play a pivotal role in revolutionizing concrete technology and fostering the development of more resilient and long-lasting infrastructure in salt-affected regions. The following conclusions were drawn from the study.

1) The compressive strength of the developed biological mortars was equivalent to that of conventional mortar.
2) When the volume fraction of expanded vermiculites immobilizing bacteria increased from 10 to 30%, the chloride ion diffusion coefficient decreased by 50–90% compared with that of control mortars without bacteria. Additionally, the viable bacterial cells in the hardened mortars increased from 6.0×10^4 cell/ml to 2.0×10^5 cell/ml.
3) The glycocalyx formation with a thickness of approximately 150 μm was observed on the surface of biological mortars containing 30% expanded vermiculites immobilizing bacteria.
4) The service life of concrete structures repaired with biological mortars containing 30% expanded vermiculites and thickness of 50 mm was expected to be six-times longer than that of the concrete structures repaired using the conventional mortar. Overall, the application of biological mortars represents a significant step towards enhancing the service life of RC structures exposed to salt attack.

Acknowledgements
This work was supported by a National Research Foundation of Korea (NRF) grant funded by the Korea Government (MSIP) (No. NRF-2020K1A3A1A05103600) and Ministry of Science and Technology of Vietnam (the research project code NDT/KR/21/19).

Author contributions
The first author, H.S. Yoon, mainly conducted the experiments and discussion of test results. The corresponding author, K.H. Yang, planned and supervised the experiments and this manuscript. The third author, S.J. Kwon, analyzed the service life of structures exposed to salt attack. The fourth author, J.W. Hwang, examined the chloride diffusion coefficient of the specimens and counted bacteria populations in the hardened coating materials. The fifth author, S.S. Lee, selected the halophilic bacteria and cultivated them in high concentrations. The sixth author, N.V. Tuan, examined the practical applicability of the developed coating materials, particularly for seashore concrete structures in Vietnam using the local materials. All authors read and approved the final manuscript.

Availability of data and materials
All data generated or analyzed during this study are included in this published article.

Declarations

Competing interests
None of the authors have any competing interests in the manuscript.

Received: 6 May 2023 Accepted: 22 October 2023
Published online: 05 March 2024

References

Andrade, C., Diez, J. M., & Alonso, C. (1997). Mathematical modeling of a concrete surface "skin effect" on diffusion in chloride contaminated media. *Advanced Cement Based Materials, 6*, 39–44.
Arya, C., Buenfeld, N. R., & Newman, J. B. (1990). Factors influencing chloride binding in concrete. *Cement and Concrete Research, 20*(2), 291–300.
Arya, C., & Xu, Y. (1995). Effect of cement type on chloride binding and corrosion of steel in concrete. *Cement and Concrete Research, 25*(4), 893–902.
ASTM C109. (2012). *Annual book of ASTM standards*. ASTM International.
Bagheri, A., Ajam, A., & Zanganeh, H. (2021). Effect of very early age exposure on chloride ingress and service life performance of binary and ternary concretes. *Construction and Building Materials, 289*, 123137. https://doi.org/10.1016/j.conbuildmat.2021.123137
Brenner, D. J., Krieg, N. R., & Staley, J. T. (2005). *Bergey's manual of systematic bacteriology* (2nd ed.). Springer.
Broomfield, J.P. (1997). Corrosion of Steel in Concrete: Understanding. *Investigation and Repair, E&FN*, London, 1–15.
Dhir, R. K., El-Mohr, M. A. K., & Dyer, T. D. (1997). Developing chloride resisting concrete using PFA. *Cement and Concrete Research, 27*(11), 1633–1639.
Diamanti, M. V., Brenna, A., Bolzoni, F., Berra, M., Pastore, T., & Ormellese, M. (2013). Effect of polymer modified cementitious coatings on water and chloride permeability in concrete. *Construction and Building Materials, 49*, 720–728.
Freshney, R. (1987). *Culture of animal cells: A manual of basic technique*. Alan R. Liss Inc.
Imhoff, J. F., Trüper, H. G., & Pfennig, N. (1984). Rearrangement of the species and genera of the phototrophic 'purple nonsulfur bacteria.' *International Journal of Systematic and Evolutionary Microbiology, 34*(3), 340–343.
Jung, S. H., Ryu, H. S., Karthick, S., & Kwon, S. J. (2018). Time and crack effect on chloride diffusion for concrete with fly ash. *International Journal of Concrete Structures and Materials*. https://doi.org/10.1186/s40069-018-0230-2
Kawasaki, H., Hoshino, Y., Hirata, A., & Yamasato, K. (1993). Is intracytoplasmic membrane structure a generic criterion? It does not coincide with phylogenetic interrelationships among phototrophic purple nonsulfur bacteria. *Archives of Microbiology, 160*, 358–362.
Kwon, S. J., Na, U. J., Park, S. S., & Jung, S. H. (2009). Service life prediction of concrete wharves with early-aged crack: Probabilistic approach for chloride diffusion. *Structural Safety, 31*(1), 75–83.
Luo, R., Cai, Y., Wang, C., & Huang, X. (2003). Study of chloride binding and diffusion in GGBS concrete. *Cement and Concrete Research, 33*(1), 1–7.
Nguyen, P. T., Bastidas-Areaga, E., Amiri, O., & Soueidy, C. P. E. (2017). An efficient chloride ingress model for long-term lifetime assessment of reinforced concrete structures under realistic climate and exposure conditions. *International Journal of Concrete Structures and Materials, 11*(2), 199–213.
Nokken, M. R., Boddy, A., Hooton, R. D., & Thomas, M. D. A. (2006). Time dependent diffusion in concrete. *Cement and Concrete Research, 36*(1), 200–207.
Petcherdchoo, A. (2015). Repairs by fly ash concrete to extend service life of chloride-exposed concrete structures considering environmental impact. *Construction and Building Materials, 98*, 799–809.
Pontes, J., Bogas, J. A., Real, S., & Silva, A. (2021). The rapid chloride migration test in assessing the chloride penetration resistance of normal and lightweight concrete. *Applied Science*. https://doi.org/10.3390/app11167251
Qian, C., Zhang, Y., & Xie, Y. (2021). Effect of ion concentration in crack zone on healing degree of microbial self-healing concrete. *Construction and Building Materials*. https://doi.org/10.1016/j.conbuildmat.2021.122969

Riding, K. A., Thomas, M. D. A., & Folliard, K. J. (2013). Apparent diffusivity model for concrete containing supplementary cementitious materials. *ACI Materials Journal, 110*(6), 705–714.
Scarfato, P., Di Maio, L., Fariello, M. L., Russo, P., & Incarnato, L. (2012). Preparation and evaluation of polymer/clay nanocomposite surface treatments for concrete durability enhancement. *Cement and Concrete Composite, 34*(3), 297–305.
Shaikh, F. U. A. (2018). Effect of cracking on corrosion of steel in concrete. *International Journal of Concrete Structures and Materials*. https://doi.org/10.14359/51731551
Thomas, M. D. A., & Bamforth, P. B. (1999). Modeling chloride diffusion in concrete: Effect of fly ash and slag. *Cement and Concrete Research, 29*, 487–495.
Thomas, M. D. A., & Bentz, E. C. (2002). *Computer Program for predicting the service life and life-cycle costs of reinforced concrete exposed to chlorides: Life365 Manual*. Silica Fume Association.
Tritthart, J. (1989). Chloride binding in cement, II. The influence of hydroxide concentration in the pore solution of hardened cement paste on chloride binding. *Cement and Concrete Research, 19*, 683–691.
van Niel, C. B. (1944). The culture, general physiology, morphology, and classification of the non-sulfur purple and brown bacteria. *Bacteriology Reviews, 8*(1), 1–118.
Wang, J., Ersan, Y. C., Boon, N., & De Belie, N. (2016). Application of microorganisms in concrete: a promising sustainable strategy to improve concrete durability. *Applied Microbiology and Biotechnology, 100*(7), 2993–3007.
Wang, Y., & Fu, K. (2019). Comparisons of instantaneous chloride diffusion coefficients determined by RCM method and chloride natural diffusion test. *Construction and Building Materials, 223*, 595–604.
Wetzel, B., Rosso, P., Haupert, F., & Friedrich, K. (2006). Epoxy nanocomposites–fracture and toughening mechanisms. *Engineering Fracture Mechanics, 73*(16), 2375–2398.
Willems, A., Gillis, M., & de Ley, J. (1991). Transfer of rhodocyclus gelatinosus to rubrivivax gelatinosus gen. nov., comb. Nov., and phylogenetic relationships with Leptothrix, *Sphaerotilus natans*, *Pseudomonas saccharophila*, and *Alcaligenes latus*. *International Journal of Systematic and Evolutionary Microbiology, 41*(1), 65–73.
Woo, R., Zhu, H., Chow, M., Leung, C., & Kim, J. (2008). Barrier performance of silane-clay nanocomposite coatings on concrete structure. *Composite Science and Technology, 68*(14), 2828–2836.
Yang, L. F., Cai, R., & Yu, B. (2017). Investigation of computational model for surface chloride concentration of concrete in marine atmosphere zone. *Ocean Engineering, 138*, 105–111.
Yang, P., Dhandapni, Y., Santhanam, M., & Neithalath, N. (2020b). Simulation of chloride diffusion in fly ash and limestone-calcined clay cement (LC3) concrete and the influence of damage on service-life. *Cement and Concrete Research, 130*, 106010. https://doi.org/10.1016/j.cemconres.2020.106010
Yang, K. H., Lim, H. S., & Kwon, S. J. (2020a). Effective bio-slime coating technique for concrete surfaces under sulfate attack. *Materials, 13*(7), 1512. https://doi.org/10.3390/ma13071512
Yang, K. H., Yoon, H. S., & Lee, S. S. (2018). Feasibility tests toward the development of protective biological coating mortars. *Construction and Building Materials, 181*, 1–11.
Yoon, H.S. 2021. Characteristics of Biomimetic Protective Coating Materials Using Bacteria Slime Immobilized by Negative Pressure for Concrete Exposed to Sulfate Attack. Ph.D. Thesis, Kyonggi University, Suwon, Korea.
Yoon, H. S., Yang, K. H., & Kwon, S. J. (2022a). Service life of sewage culver with bacteria coating from waste sludge and negative pressure method. *Journal of Material Cycles and Waste Management, 24*, 582–594.
Yoon, H. S., Yang, K. H., & Lee, S. S. (2021). Evaluation of sulfate resistance of protective biological coating mortars. *Construction and Building Materials, 270*, 1–9.
Yoon, H. S., Yang, K. H., Lee, S. S., & Hwang, J. W. (2022b). Effect of halophilic bacteria on reducing chloride-ion concentration in mortars. *Construction and Building Materials, 351*, 1–10. https://doi.org/10.1016/j.conbuildmat.2022.128918
Yoon, I. S., & Saeki, T. (2021). Mechanism of chloride ion adsorption in cement hydrates as per time-dependent behavior. *ACI Materials Journal, 118*, 41–53.
Yuan, Q., Shi, C., De Schutter, G., Audenaert, K., & Deng, D. (2009). Chloride binding of cement-based materials subjected to external chloride environment – A review. *Construction and Building Materials, 23*(1), 1–13.
Zahn, Q., Dong, W., Fu, C., Wang, A., Yi, H., & Pan, Z. (2022). The self-healing of marine concrete cracks based on the synergistic effect of microorganisms and inorganic minerals. *Journal of Building Engineering, 61*, 105210. https://doi.org/10.1016/j.jobe.2022.105210
Zhang, Y., Zhou, X. Y., Zhao, J., Zhuang, H. X., Gao, Y. H., & Zhang, Y. R. (2019). Time dependency and similarity of decay process of chloride diffusion in concrete under simulated marine tidal environment. *Construction and Building Materials, 205*, 332–343.

Publisher's Note

Hyun-Sub Yoon is a Chief Technology Officer (CTO) of Korea Disaster Prevention Safety Technology Co., Ltd. His research interests on the development of functional concrete and mortar using bacteria.

Keun-Hyeok Yang is a professor at Kyonggi University, South Korea. He received the Scientific Technician Medal for Most Meritorious Achievement in 2010 from the National Research Foundation of Korea. His recent research interests include the development of sustainable concrete materials and structural technology.

Seung-Jun Kwon is an Associate Professor at Hannam University, Daejeon, South Korea. His research interests include modeling of microstructure and deterioration analysis in cement composites using neural network algorithms and strengthening techniques for concrete structures.

Ji-Won Hwang is a graduate student at Kyonggi University, South Korea. Her interest focuses on developing functional concrete and mortars utilizing bacteria.

Sang-Seob Lee is a professor at Sungkyunkwan University, South Korea. He is a Director of The Korea Environmental Mircroorganisms and Gene Core Center supported by Korean government. His recent research interests include the development and practical application of functional microorganisms.

Nguyen Van Tuan is an Associate Professor at Hanoi University of Civil Engineering, Hanoi, Vietnam. His research interests include the hydration, microstructure, and durability of sustainable concrete materials using mineral admixtures, especially based on ultra-high performance concrete technology.